

1 **Wildfire-derived pyrogenic carbon modulates organic matter**
2 **and microbial functioning in a fluvial ecosystem**

3 Lukas Thuile Bistarelli,¹ Caroline Poyntner,² Cristina Santín,^{3,4} Stefan H. Doerr,⁵ Matthew
4 V. Talluto,¹ Gabriel Singer,¹ Gabriel Sigmund^{6*}

5

6 ¹ Institute of Ecology, University of Innsbruck, Technikerstraße 25, 6020 Innsbruck, Austria

7 ² Institute of Microbiology, University of Innsbruck, Technikerstraße 25, 6020 Innsbruck, Austria

8 ³ Research Unit of Biodiversity, Spanish National Research Council (CSIC), Mieres, Spain

9 ⁴ Swansea University, Department of Biosciences, Singleton Park, Swansea SA2 8PP, UK

10 ⁵ Swansea University, Department of Geography, Singleton Park, Swansea SA2 8PP, UK

11 ⁶ University of Vienna, Department of Environmental Geosciences, Centre for Microbiology and
12 Environmental Systems Science, Althanstraße 14, 1090 Wien, Austria

13

14

15

16 **Corresponding author:** Gabriel Sigmund University of Vienna, Department of Environmental
17 Geosciences, Centre for Microbiology and Environmental Systems Science, Althanstraße 14,
18 1090 Wien, Austria e-mail: gabriel.sigmund@univie.ac.at

19 **Abstract**

20 Wildfires produce large amounts of pyrogenic carbon (PyC), including particulate
21 charcoal, known for its chemical recalcitrance and sorption affinity for organic molecules.
22 Wildfire-derived PyC is highly mobile in the landscape and can be transported to fluvial
23 networks where it may impact natural dissolved organic matter (DOM) and microbial
24 biofilms. The effects of PyC on freshwater ecosystems and carbon cycling therein remain
25 poorly investigated. To address this research gap, we used in-stream flumes with a
26 control vs treatment design (pulse addition of PyC particles). We present evidence that
27 field-aged PyC inputs into river ecosystems can alter dissolved organic carbon (DOC)
28 concentration, DOM composition, pH, and enzymatic activities in benthic biofilms. In-
29 stream DOM composition was altered due to leaching of pyrogenic DOM from PyC and
30 possible concurrent sorption of riverine DOM to PyC. DOM changes and increase in pH
31 were associated with changes in enzymatic activities, which reflected preferential usage
32 of recalcitrant over easily available DOM by biofilms. Furthermore, we observed
33 particulate PyC sedimentation on biofilm surfaces, which may further modulate the
34 impacts of PyC. This study highlights the importance of PyC for in-stream DOM properties
35 and biofilm functioning with implications for in-stream biogeochemical cycling in fire-
36 affected watersheds.

37 **Keywords**

38 Pyrogenic carbon; dissolved organic matter; biofilm functioning; enzymatic activities;

39 **1. Introduction**

40 Vegetation fires annually burn ~4 % of Earth's vegetated land surface, forming
41 approximately 256 Tg of pyrogenic carbon (PyC).¹ PyC is a continuum of thermally-
42 altered organic materials including charcoal, of which a considerable fraction is highly
43 recalcitrant, persisting in the environment for prolonged periods of time.² In fire-affected
44 landscapes fresh as well as aged PyC is continuously mobilized to fluvial ecosystems via
45 water erosion (e.g. surface runoff).³⁻⁵ Coppola and colleagues⁶ found that globally $15.8 \pm$
46 0.9% of riverine particulate organic carbon is of pyrogenic origin. Jones and colleagues⁷
47 estimated that PyC accounts for $12 \pm 5\%$ of the riverine dissolved organic carbon (DOC,
48 i.e., filtered $< 0.45 \mu\text{m}$).

49 Rivers do not only transport but also transform organic matter on its way downstream
50 towards the ocean via photochemical and microbial processes in the water column.⁸⁻¹⁰
51 Photo-chemical reactions, which are strongly site dependent,¹¹ can preferentially degrade
52 aromatic compounds deriving from pyrogenic sources.¹² In-stream microbiota, especially
53 biofilm communities which are hotspots of microbial functioning, are central to the role of
54 fluvial ecosystems as bioreactors of terrestrial material.¹³

55 The non-recalcitrant, more labile fraction of PyC can be a relevant component of in-
56 stream carbon turnover.^{14,15} Changes in DOC quantity and DOM composition induced by
57 PyC may alter microbial functioning, based on observations in non-fire affected aquatic
58 systems.^{9,16,17} PyC particles can interact with the riverine DOM via selective adsorption,
59 thus affecting DOM composition and susceptibility to microbial metabolism. This process
60 has previously been observed for other carbonaceous materials, including carbon-

61 nanomaterials,^{18,19} graphite, and biochar.¹⁹ PyC can also disintegrate into smaller
62 particles, and leach organic matter as well as metals.^{20–22}

63 Here we report on a field experiment in a natural river to investigate the effects of wildfire-
64 derived PyC inputs on in-stream DOM properties and biofilm functioning. We
65 hypothesized that PyC would affect (i) in-stream DOM composition and DOC
66 concentration due to sorption of riverine DOM and leaching of pyrogenic DOM, and (ii)
67 microbial functions, measured via enzymatic activities.

68 **2. Methods**

69 **2.1 Site description and field experimental design**

70 This study was carried out at the Austrian river Kleine Ysper (lat 48.218N, long 15.023E),
71 a tributary of the Ysper with a slope of 3.3 cm/m, situated about 4 km upstream of the
72 confluence with the Danube. This site was selected because the land use in its catchment
73 area is dominated by mixed forest and semi-natural areas which are widespread in the
74 region, and the site has already been characterized in a previous study.²³ The wildfire-
75 derived PyC used was woody charcoal collected one year after an extensive wildfire in a
76 pine forest (*Pinus sylvestris*, Karbole, Sweden), sieved to 5 – 10 mm and homogenized.
77 The PyC's molar carbon to nitrogen (C/N) ratio was measured in triplicates on a CHNS
78 analyzer (Vario MACRO, Elementar).

79 For the experiment, 60 ceramic tiles of 25 cm² fixed to a wooden board were exposed on
80 the riverbed from 14th June 2019 to 12th July 2019 for colonization by biofilm communities.
81 On 12th July 2019, a total of ten experimental in-situ flumes built from commercially
82 available 20-l boxes were placed in the river. Inflow of river water into the flumes was
83 provided using 6 m long tubing (8 mm inner Ø) for each box, whose inflow was placed
84 upstream of the flumes at a hydraulic head of 20 cm, resulting in an average discharge
85 of 0.47 ± 0.01 l min⁻¹. Tiles from the river were randomly distributed across the flumes
86 (Fig. 1). Five flumes were used as treatment and control flumes, respectively. 15 paper-
87 filter bags, each containing 15 g of particulate PyC, were added to each treatment flume
88 at the start of the experiment. The filter bags had a mesh size < 50 µm to allow the release
89 of small PyC particles and DOC. In the control flumes, filter bags without PyC were added
90 to account for potential riverine DOM interactions with the filter bag.

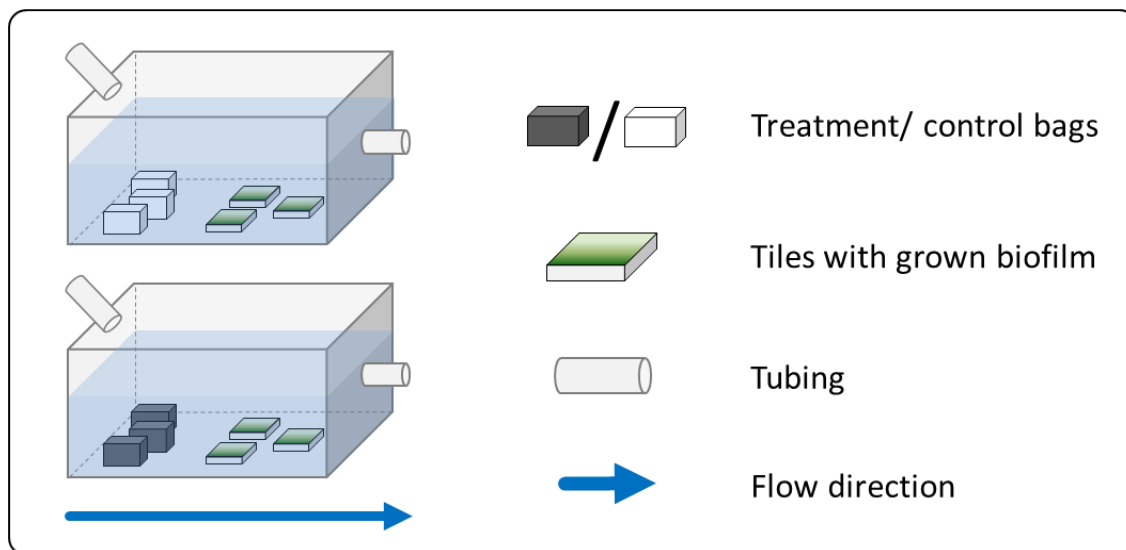


Figure 1: Stream-side flumes setup. Flume design showing bags filled with inert quartz sand (upper) and PyC (lower) for control and treatment, respectively.

91 Water samples were collected at each outflow 1, 2, 3, 4, 6, and 8 h after the beginning of
92 the experiment. Additionally, we monitored O₂, pH, and conductivity using a WTW probe
93 (Xylem, Germany). At 1, 4, and 8 h samples were taken for the measurement of total

94 concentrations of Li, Na, Mg, Al, Ca, Sc, Mn, Fe, Co, Zn, Rb, Sr, Y, Mo, Ba, La, Ce, Pr,
95 Nd, Sm, Gd, Dy, Pb, and U (see Figure S1 and Table S1 in the Supporting Information
96 for details). For light microscopical analysis of particulate PyC sedimentation on biofilm
97 surfaces, 20 microscopic glass slides were placed at the bottom of the flumes for the
98 duration of the experiment (see Supporting Information for details).

99 Due to sedimentation and partial dilution, it was not possible to quantify the leached
100 particulate organic carbon fraction in the flume setup. To overcome this issue, we
101 performed complementary leaching experiments in the lab for the duration of the flume-
102 experiment using river water (8 h, see Table S2 in the Supporting Information for details).

103 **2.2 Organic matter properties**

104 To determine DOC concentration and DOM properties, water samples were sterile filtered
105 through pre-washed 0.2 μm Minisart syringe filters (Sartorius, Germany) into 2 ml HPLC
106 vials (acidified with ultrapure HCl to pH = 2) for DOC and 10 ml glass vials with PTFE
107 septa for DOM analyses. DOC was analyzed by high temperature combustion on a multi
108 N/C 2100s (Analytik Jena, Germany). DOM samples were analyzed
109 spectrofluorometrically on a Horiba Aqualog (Horiba Ltd, Japan), which measures
110 absorbance (250-600 nm, 5 nm increment) and excitation-emission matrices (EEMs,
111 excitation 250-550 nm, emission 250-600 nm, 5 nm increment) concomitantly using a 1
112 cm quartz cuvette and MilliQ (Millipore, United States) water as optical blank.

113 The decadal absorption coefficient at 254 nm was used to compute specific UV
114 absorption (SUVA_{254}) which commonly serves as a proxy for aromaticity.²⁴ SUVA_{254} was
115 also determined for leachates from PyC particles in MilliQ water incubated for 24 h.

116 Rayleigh scatter was deleted from EEMs and Raman scatter was removed by subtracting
117 MQ EEMs from samples EEMs.^{25,26} EEMs were used for parallel factor analysis
118 (PARAFAC)^{27,28} using the R package stardom.²⁹ After exclusion of outliers, 54 EEMs
119 were used to derive 4 fluorescent components, which were compared with literature using
120 the online database OpenFluor.

121 **2.3 Potential extracellular enzymatic activity**

122 Biofilm grown on the submerged tiles was used to perform the potential extracellular
123 enzymatic activity (EEAs) assays reflecting the maximum capacity of an enzyme to cleave
124 a given substrate. We measured the activity of the enzymes β -glucosidase (EC 3.2.1.21),
125 β -xylosidase (EC 3.2.1.37), cellobiohydrolase (EC 3.2.1.91), β -N-acetylglucosaminidase
126 (EC 3.2.1.30), phosphatase (EC 3.1.3.1-2), lipase (EC 3.1.1.3), leucine-aminopeptidase
127 (EC 3.4.11.1), and phenol oxidase (EC 1.10.3). These enzymes are broadly used to
128 understand effects of DOM on bacterial community functioning.^{17,30–37} Enzyme assays
129 were prepared beforehand in deep well plates and brought to the field frozen. At the end
130 of the 8 h field-experiment, we scraped off the biofilm from the submerged tiles using a
131 scalpel and subsequently homogenized it using a frother. The biofilm slurry was used to
132 inoculate the assay which was incubated for 1 h at dark and river temperature. Thereafter,
133 the process was stopped using buffers, and plates were immediately frozen on site. After
134 two days, the plates were thawed, gently centrifuged, and analyzed in the laboratory on
135 a Spark plate-reader (Tecan Trading AG, Switzerland). Measured enzymatic activities
136 were used to compute enzymatic activity ratios (ERs) as these are biomass independent.
137 Further experimental details can be found in the Supporting Information.

138 2.4 Statistical analysis

139 To analyze DOC and DOM data, we applied Gaussian process (GP) regressions as they
140 are able to account for the nonindependence in the response variables that results from
141 the repeated measurements over time. GP regression employs a flexible model structure
142 that can describe the effects of predictors on both the mean and the (auto-) covariance
143 structure of the response variable.³⁸ We employed a simple linear equation for the mean
144 function:

$$145 \quad E(y) = \alpha + \beta * T \quad \text{eq (1)}$$

146 where T is an indicator variable indicating whether the treatment was applied; with no
147 covariance and constant variance, this model is nearly identical to a simple linear
148 regression with a categorical predictor.

149 We modelled covariance within flumes as a decaying function of observation time using
150 a Gaussian kernel function:

$$151 \quad \text{cov}(y_1, y_2) = \alpha^2 \exp\left(-\frac{(t_1 - t_2)^2}{2\rho^2}\right) + \delta_{ij} \sigma^2 \quad \text{eq (2)}$$

152 where α and ρ are hyperparameters controlling the variance and bandwidth of the
153 Gaussian process, δ_{ij} is an indicator that is 1 if $i = j$ and 0 otherwise, σ^2 is the residual
154 variance of the response variable y and t is the time of measurement. This kernel
155 generates a variance-covariance matrix where covariance increases as the time between
156 a pair of observations decreases, thus accounting for any autocorrelation due to the
157 repeated measures design of the experiment. We assumed covariance among flumes
158 was zero, and we calibrated a single set of hyperparameters (i.e., α , ρ , and σ) for all

159 flumes, thus assuming that the strength of the time-covariance relationship was identical
160 among flumes. We calibrated the model using the package rstan.³⁹ We also compared
161 the results of the GPs to generalized linear models (GLMs) with no time dependence and
162 obtained similar parameter estimates. Differences between enzyme ratios in treatment
163 and control flumes were analyzed using t-tests as these data were collected exclusively
164 at the end of the experiment. All uncertainty estimates are provided as standard errors.

165 **3. Results & Discussion**

166 **3.1 Pyrogenic carbon increases pH and dissolved organic carbon**

167 pH was elevated by approximately 0.25 units in the treatment flumes compared to the
168 controls after the first 3 h of the experiment and remained nearly constant throughout the
169 8 h experiment (see Fig. S2a in the Supporting Information). In contrast, O₂ content and
170 conductivity were not strongly affected by PyC addition (see Fig. S2 in the Supporting
171 Information). This is in good agreement with the well-documented alkalinity of biochar –
172 an engineered PyC primarily used in agricultural applications. This alkalinity derives from
173 alkaline surface functional groups on the aromatic PyC structure, as well as carbonates,
174 and other inorganic moieties in the ash fraction.^{40,41} Metals, which can occur in the ash
175 fraction, are known to interfere with the functioning of microbial cells by blocking the active
176 center of enzymes.²⁰ However, our results indicate that PyC only slightly affected the
177 concentration of 3 out of 24 metals quantified (see Fig. S1 and Table S1 in the Supporting
178 Information). This may be because the PyC used was one year old prior to its deployment
179 in our experiment and, therefore, was depleted from the easily dissolvable ash fraction
180 during field aging. A slight increase in aqueous concentration was observed for Mn and

181 Rb, which were likely released from the PyC. The aqueous concentration of Zn decreased
 182 in the presence of PyC, which is consistent with previous reports on the immobilization of
 183 Zn by engineered pyrogenic materials such as biochar.⁴²

184 DOC concentrations across all time points ranged from 2.61 to 4.17, and 2.97 to 7.06 mg
 185 l⁻¹ in the control and treatment flumes, respectively. Overall, DOC concentration slightly
 186 increased with PyC addition (Fig. 2a, 2b). DOC concentrations were higher in the
 187 treatment (mean predicted DOC 3.72 ± 0.14 mg l⁻¹) in comparison to the control (mean
 188 predicted DOC 3.32 ± 0.14 mg l⁻¹) flumes, with an overall effect size of 0.4 mg l⁻¹ based
 189 on Gaussian process regression (Fig. 2b). The increases in DOC concentration in
 190 treatment flumes can be explained by leaching of pyrogenic organic matter from wildfire
 191 charcoals, as also observed in previous laboratory studies.^{43,44} Our results indicate that
 192 DOC-leaching from PyC exceeds the adsorption of riverine DOC to PyC under conditions
 193 such as the ones studied here.

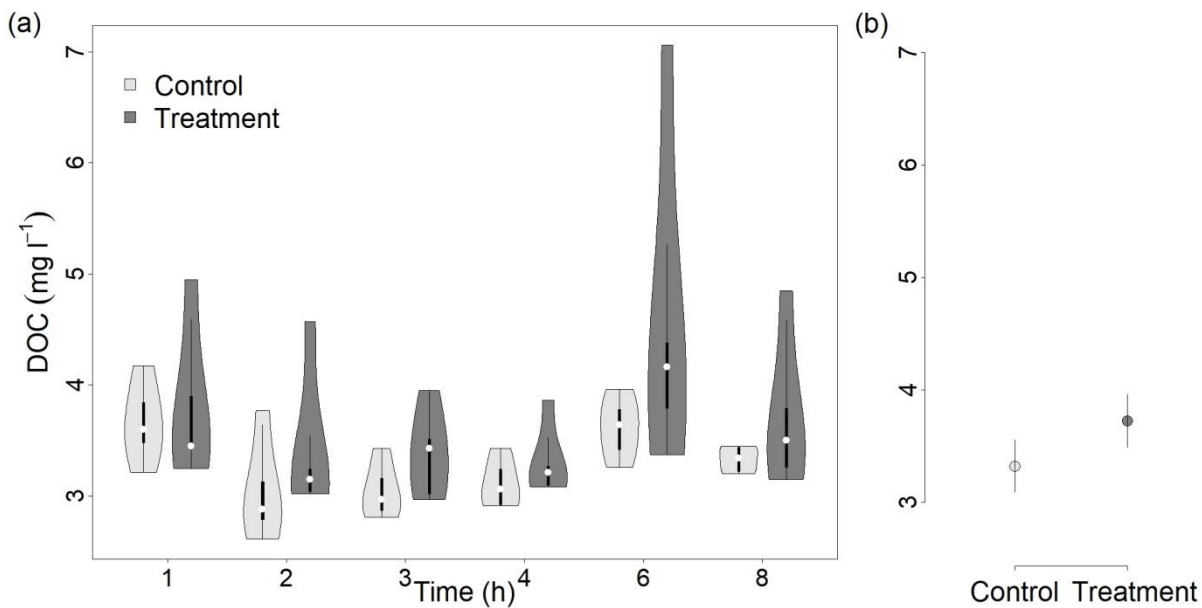


Figure 2: a) DOC concentrations over time in the control and treatment flumes. White dot in box-plots represents median values. b) Mean predicted DOC concentrations based on Gaussian process models for control (light grey) and treatment (dark grey) flumes with 90 % CI.

194 The amount of DOC released from filter bags in the field experiments was estimated as:

$$195 \quad DOC_{leached} = \frac{Q \cdot t \cdot \Delta DOC}{n} \quad \text{eq (3)}$$

196 where Q is the flume-discharge, t the duration of the experiment, ΔDOC the modelled
197 treatment effect, and n the number of filter bags in each flume. These calculations indicate
198 that 5.99 ± 0.02 mg DOC were leached from each filter bag over the 8 h duration of the
199 experiment.

200 Under laboratory conditions each filter bag released 12.64 ± 0.12 mg C total organic
201 carbon (TOC) over 8 h (see Table S2 in the Supporting Information for details). Based on
202 these results, particulate organic carbon (POC) also increased upon wildfire char addition.
203 This suggests that small particles from the wildfire charcoal are mobilized into river water,
204 which was confirmed by the visual sedimentation of small PyC particles on the biofilm at
205 the end of the field experiment (see Fig. S3 in the Supporting Information).

206 Thus, mean POC (TOC - DOC) and DOC inputs were similar in size amounting to
207 approximately 6.65 and 5.99 mg C per filter bag, respectively. These results show that a
208 considerable amount of carbon can be released from aged PyC particles. Considering
209 that the physical stress on PyC due to water turbulence was greater during field
210 experiments compared to laboratory experiments, an even higher amount of TOC could
211 have been released in the flume experiments. The large number of particles that settled
212 on the biofilm as observed microscopically (see Fig. S3 in the Supporting Information)
213 may additionally increase PyC effects on enzymatic activity, e.g., through direct
214 interaction with the biofilm matrix.

215 3.2 Pyrogenic carbon addition changes DOM composition

216 SUVA₂₅₄, which correlates strongly with aromaticity,²⁴ ranged from 3.09 to 4.71 in the
217 control, and from 1.75 to 4.41 in the treatment flumes. Hence, SUVA₂₅₄ was consistently
218 reduced in presence of PyC, as confirmed by gaussian process regression, which found
219 lower SUVA₂₅₄ in the treatment flumes (mean predicted SUVA₂₅₄ = 3.53 ± 0.11) in
220 comparison to the control flumes (mean predicted SUVA₂₅₄ = 3.84 ± 0.11) with an overall
221 effect size of -0.31 (Fig. 3).

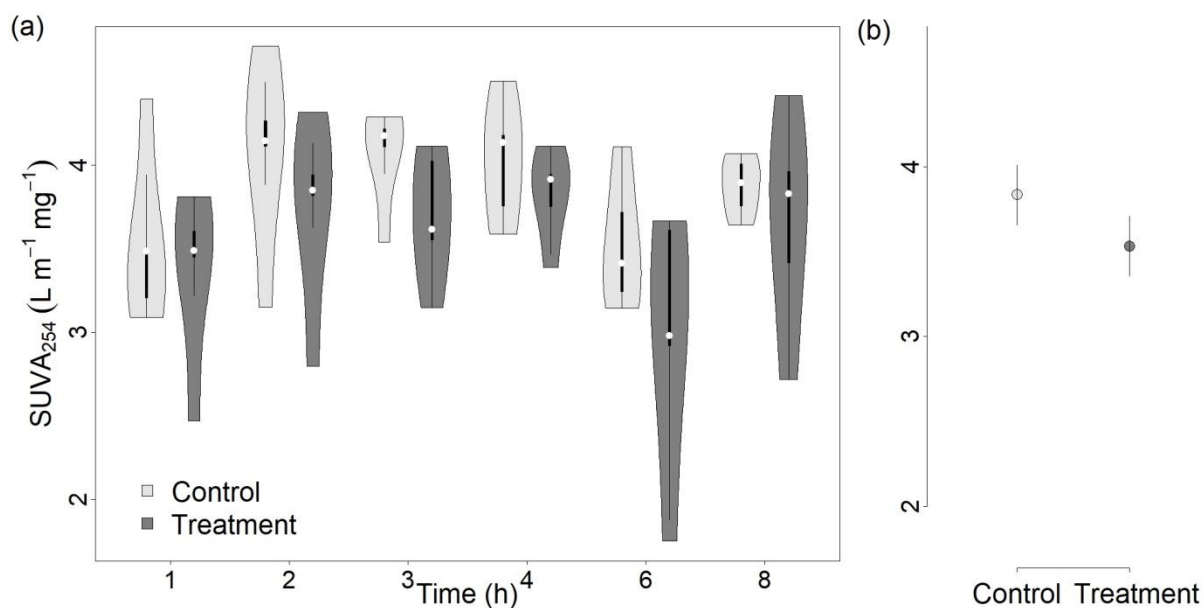


Figure 3: a) SUVA₂₅₄ over time in the control and in the treatment flumes. b) Mean predicted SUVA₂₅₄ based on Gaussian process models for control (light grey) and treatment (dark grey) flumes with 90 % CI.

222 PyC consists of labile and recalcitrant fractions, with the labile fraction being less aromatic
223 and more easily mobilized and degraded by microbes.⁴⁴ In contrast, the recalcitrant
224 fraction is expected to stay in the particulate form constituting a strong sorbent for other
225 aromatic DOM compounds. Our hypothesis that leaching of labile compounds with low
226 aromaticity from PyC occurs, is supported by low SUVA₂₅₄ values (1.78 ± 0.35) in MilliQ
227 water leaching experiments. The reduced SUVA₂₅₄ values in treatment flumes (Fig. 3)
228 could additionally suggest that selective sorption of riverine DOM by PyC simultaneously

229 removed aromatic compounds from the water. The SUVA₂₅₄ measurements are in line
230 with recent studies showing that sorption of DOM to PyC particles increases with DOM
231 aromaticity and can be hindered by steric effects excluding very large DOM molecules
232 from reaching certain sorption sites within the charcoal particles.^{19,45}

233 PARAFAC, a modelling approach used to unravel chemical signatures from EEMs,
234 resulted in the detection of 4 components (see Fig. 4 and OpenFluor PARAFAC report
235 (<https://openfluor.lablicate.com/of/measurement/2604>)). No significant differences were
236 observed due to PyC additions in any of the 4 components (see Fig. S4 in the Supporting
237 Information).

238 C1, C2, and C3 are humic-like components whereas C4 is a protein-like component.^{25,46–}
239 ⁵⁰ C2 is possibly microbial humic-like based on results from Yamashita and colleagues.⁵¹
240 Although not clearly detectable, PARAFAC components suggest that there was a slight
241 increase of mostly humic like chemical compounds following PyC addition (see Fig. S4 in
242 the Supporting Information). This notion is supported by the measured total fluorescence
243 (see Fig. S5 in the Supporting Information) which slightly increased due to PyC addition.
244 However, further investigation into PARAFAC components from similar experiments at
245 larger scales and possibly increased PyC concentrations are needed to confirm these
246 interpretations.

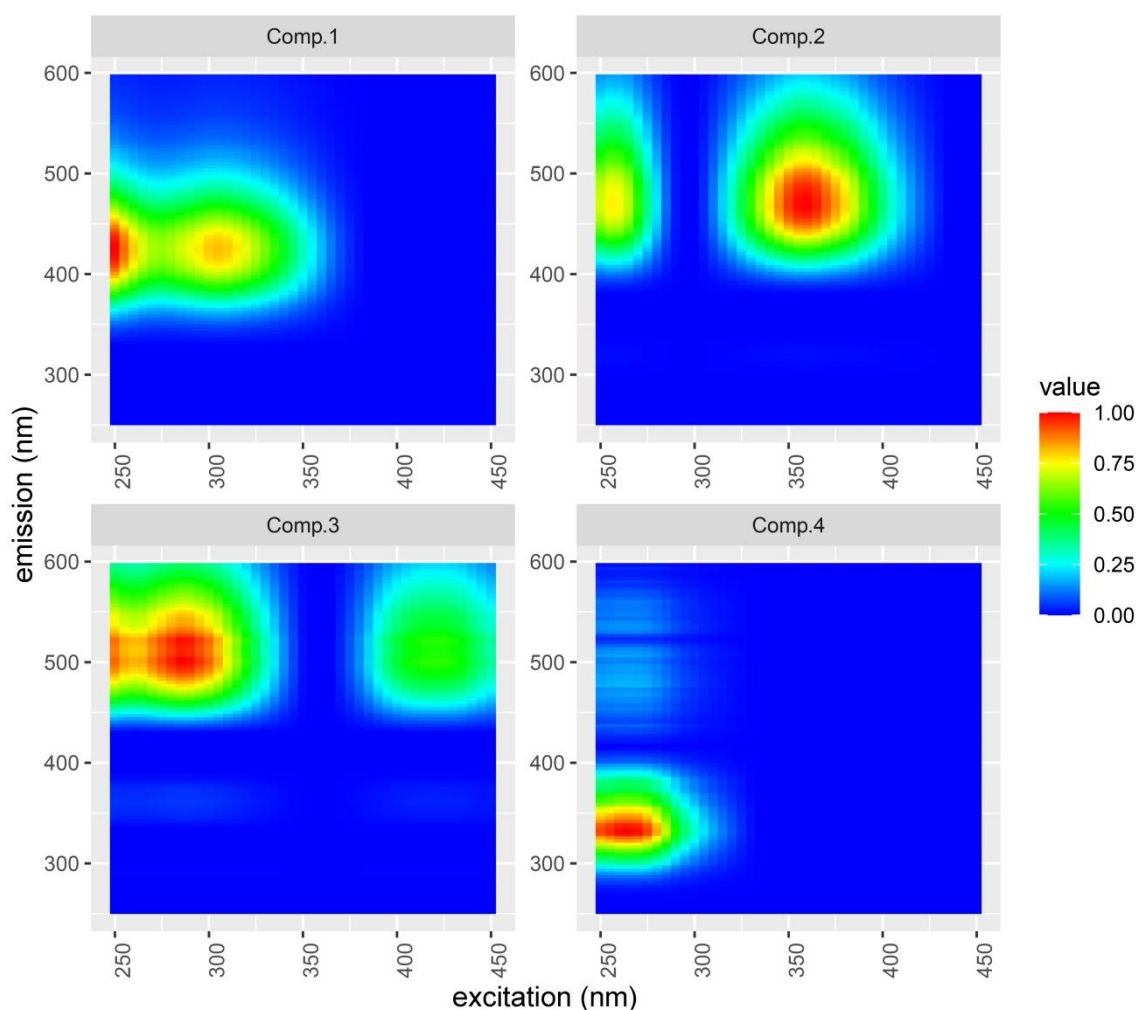


Figure 4: Excitation emission matrices (EEMs) for all four PARAFAC components, modelled from all samples. C1 has its excitation maximum at 250nm and emission maximum at 425nm. C2 has its excitation peak at 360nm and emission peak at 465nm. C3 and C4 have their excitation peak at 285 and 265nm and their emission peaks at 500 and 335nm respectively.

247 **3.3 Pyrogenic carbon addition affects enzymatic activities**

248 Oxidation and hydrolysis are two key processes for DOM degradation. Hydrolytic
 249 enzymes degrade non-aromatic DOM structures and oxidative enzymes also degrade
 250 aromatic DOM structures.⁵² PyC more strongly affected enzymatic activity ratios (ERs)
 251 with phenol oxidase (Pox, the only oxidative enzyme investigated) compared to hydrolytic
 252 enzymes (see Fig. 5 and Fig. S6 in the Supporting Information).

253 The ERs Xyl/Glu, (Glu+Xyl)/Cbh, Glu/Pox and NAG/Pox, were affected by PyC addition
254 (Fig. 5). Xyl/Glu increased upon PyC addition (t-test, d.f.= 4, p=0.03), indicating a
255 preferential use of large polymeric carbon compounds in comparison to the control
256 flumes. The ratio (Glu+Xyl)/Cbh slightly decreased with PyC addition (t-test, d.f.= 4,
257 p=0.08), indicating a reduced use of easily available polysaccharides in comparison to
258 complex polysaccharides. Glu/Pox, also referred to as the recalcitrance index, decreased
259 with PyC addition (t-test, d.f.= 4, p=0.03), pointing to an increase in the use of
260 polyphenolic lignin-like compounds in comparison to easily available compounds such as
261 cellobiose or small oligomers.³² Similarly, NAG/Pox decreased with PyC addition (t-test,
262 d.f.= 4, p=0.03), indicating an increased use of polyphenolic lignin-like compounds over
263 chitin-derived compounds. Furthermore, the ER variability decreased following PyC
264 addition, especially for ERs including phenol oxidase (Fig. 5c, d).

265 Observed differences of ERs in benthic biofilms can be explained by the combined effect
266 of changes in DOC quantity, DOM quality, and pH. These findings are in line with studies
267 on possible drivers of ER variability.^{17,30,33,53} For instance, in a meta-analysis comparing
268 terrestrial, marine, and freshwater ecosystems Arnosti and colleagues⁵³ found that pH is
269 more important in controlling enzymatic activities in freshwater ecosystems in comparison
270 to marine environments. Freixa and colleagues¹⁷ relate enzymatic activities in a
271 longitudinal river continuum to the change in DOM composition from up – to downstream
272 and found that enzymatic activities reflect a transition from allochthonous to
273 autochthonous DOM along the river continuum. In this study, ERs may have additionally
274 been influenced by the presence of small PyC particles on the biofilm surface due to
275 sedimentation (see Fig. S3 in the in the Supporting Information). Therein, particulate

276 bound aromatic OM may have induced an increased activity of Pox (Fig. 5 c+d) compared
277 to purely hydrolytic ERs (Fig. 5 a+b).

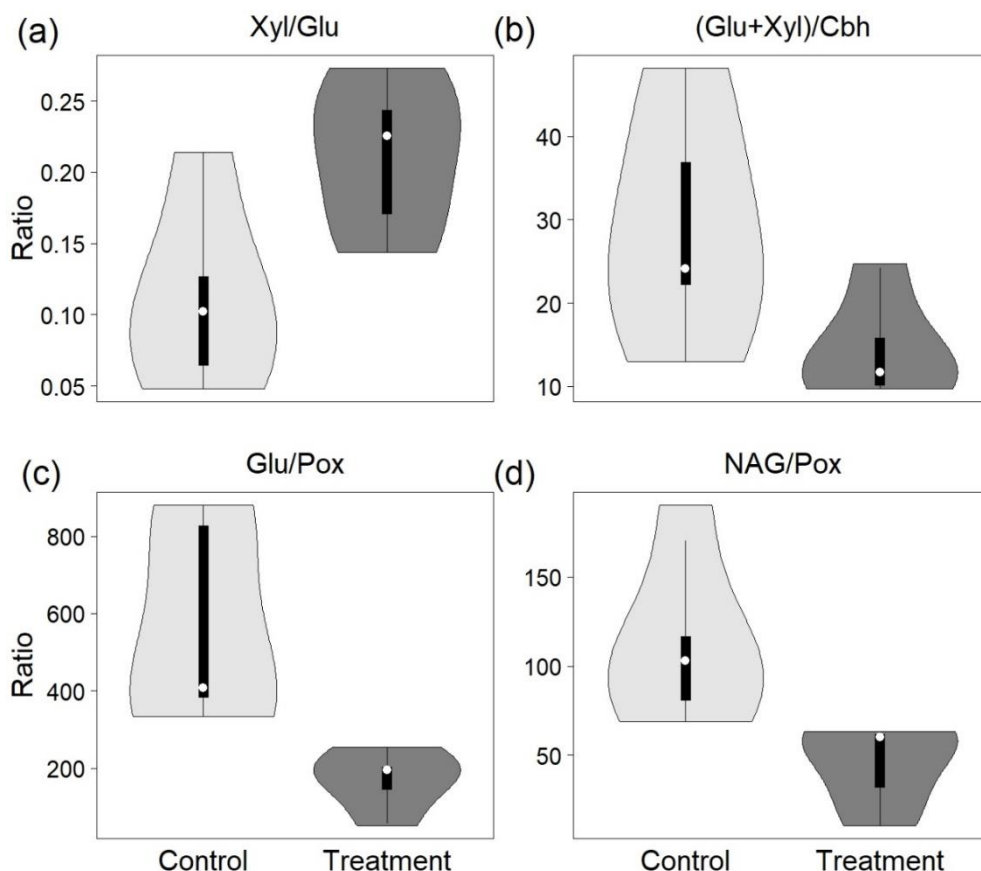


Figure 5: Enzyme ratios without (light grey) and with (dark grey) PyC addition. (a) Xyl/Glu ratio; (b) (Glu+Xyl)/Cbh ratio; (c) Glu/Pox ratio i.e. recalcitrant index; (d) NAG/Pox ratio.

278 The ERs in this study indicate that PyC addition resulted in an overall compositional
279 change of DOM towards lower biodegradability, despite an observed increase in DOC
280 (Fig. 2). It may appear contradictory that upon PyC addition, ERs indicate a decrease in
281 easily assimilable DOM while SUVA₂₅₄ indicates a decreased DOM aromaticity (Fig. 3).
282 Aromaticity, however, is not the only DOM property linked to recalcitrance and decreased
283 degradability. For instance, molecular size, aqueous solubility, oxidation state, molecular
284 complexity, as well as the lack of N-containing substituents are also linked to the
285 recalcitrance of organic matter.⁵⁴ Furthermore, the particulate PyC had a high molar C/N

286 ratio of 189 ± 24 which can be related to high recalcitrance and inaccessibility to
287 decomposers.^{54,55}

288 Our results suggest that in this experiment the input of PyC, whilst increasing DOC
289 concentrations, could curb in-stream carbon cycling. This notion is also supported by the
290 observed increase of Xyl/Glu ratios, which indicates an elevated use of hemicellulose
291 compounds over cellulose upon PyC addition (Fig. 5a). ERs suggest that PyC additions
292 can alter fluvial carbon cycling, albeit magnitude and transferability of our results needs
293 further investigation, especially in other rivers and at larger regional scales.

294 **4. Implications**

295 Surface runoff and colloidal transport of PyC into limnic systems can introduce substantial
296 changes in DOC concentration and DOM composition. We here report the release of
297 organic matter from PyC with the potential simultaneous selective adsorption of native
298 aromatic substances from riverine DOM in a natural river system. Our results indicate that
299 PyC, both in particulate and dissolved form, affect enzymatic activities in benthic biofilms
300 – especially for oxidative enzymes. PyC addition increased pH, which can also play a role
301 in altering enzymatic activities. Lastly, deposition of particulate PyC directly on the biofilm
302 surface brings the PyC in close contact with the biofilm matrix, potentially modulating the
303 aforementioned effects. Overall, our results suggest that PyC inputs into freshwater can
304 directly affect enzymatic activities, thus altering in-stream benthic biofilm functioning and
305 carbon cycling. Our in-stream flume approach applied here for the first time, could be
306 adapted to study a diverse range of rivers, enabling a more comprehensive understanding
307 of wildfire effects on riverine carbon cycling.

308 **Acknowledgement**

309 This study was partially funded within the ERC Starting Grant FLUFLUX (grant number
310 ERC-STG 716196 to GSinger). PyC sample collection was supported by FORMAS grant
311 FR-2019/0007 (CSantin & SHDoerr). We would like to thank Tobias Goldhammer and
312 Sarah Krocker of the chemical laboratory (CAB) at the Leibniz-Institute of Freshwater
313 Ecology and Inland Fisheries (IGB) for measuring DOC concentrations. We would like to
314 thank the University of Natural Resources and Life Sciences, Department of
315 Biotechnology, for using their microscope equipment.

316 **References**

- 317 (1) van der Werf, G. R.; Randerson, J. T.; Giglio, L.; van Leeuwen, T. T.; Chen, Y.;
318 Rogers, B. M.; Mu, M.; van Marle, M. J. E.; Morton, D. C.; Collatz, G. J.; Yokelson,
319 R. J.; Kasibhatla, P. S. Global Fire Emissions Estimates during 1997–2016. *Earth*
320 *Syst. Sci. Data* **2017**, *9* (2), 697–720. <https://doi.org/10.5194/essd-9-697-2017>.
- 321 (2) Jones, M. W.; Santín, C.; van der Werf, G. R.; Doerr, S. H. Global Fire Emissions
322 Buffered by the Production of Pyrogenic Carbon. *Nat. Geosci.* **2019**, *12* (9), 742–
323 747. <https://doi.org/10.1038/s41561-019-0403-x>.
- 324 (3) Santín, C.; Doerr, S. H.; Kane, E. S.; Masiello, C. A.; Ohlson, M.; de la Rosa, J. M.;
325 Preston, C. M.; Dittmar, T. Towards a Global Assessment of Pyrogenic Carbon from
326 Vegetation Fires. *Glob. Chang. Biol.* **2016**, *22* (1), 76–91.
327 <https://doi.org/10.1111/gcb.12985>.
- 328 (4) Dittmar, T.; de Rezende, C. E.; Manecki, M.; Niggemann, J.; Coelho Ovalle, A. R.;

- 329 Stubbins, A.; Bernardes, M. C. Continuous Flux of Dissolved Black Carbon from a
330 Vanished Tropical Forest Biome. *Nat. Geosci.* **2012**, *5* (9), 618–622.
331 <https://doi.org/10.1038/ngeo1541>.
- 332 (5) Bellè, S.-L.; Berhe, A. A.; Hagedorn, F.; Santin, C.; Schiedung, M.; van Meerveld,
333 I.; Abiven, S. Key Drivers of Pyrogenic Carbon Redistribution during a Simulated
334 Rainfall Event. *Biogeosciences Discuss.* **2020**, *2020*, 1–35.
335 <https://doi.org/10.5194/bg-2020-361>.
- 336 (6) Coppola, A. I.; Wiedemeier, D. B.; Galy, V.; Haghypour, N.; Hanke, U. M.;
337 Nascimento, G. S.; Usman, M.; Blattmann, T. M.; Reisser, M.; Freymond, C. V.;
338 Zhao, M.; Voss, B.; Wacker, L.; Schefuß, E.; Peucker-Ehrenbrink, B.; Abiven, S.;
339 Schmidt, M. W. I.; Eglinton, T. I. Global-Scale Evidence for the Refractory Nature
340 of Riverine Black Carbon. *Nat. Geosci.* **2018**, *11* (8), 584–588.
341 <https://doi.org/10.1038/s41561-018-0159-8>.
- 342 (7) Jones, M. W.; Coppola, A. I.; Santin, C.; Dittmar, T.; Jaffé, R.; Doerr, S. H.; Quine,
343 T. A. Fires Prime Terrestrial Organic Carbon for Riverine Export to the Global
344 Oceans. *Nat. Commun.* **2020**, *11* (1), 2791. [https://doi.org/10.1038/s41467-020-](https://doi.org/10.1038/s41467-020-16576-z)
345 [16576-z](https://doi.org/10.1038/s41467-020-16576-z).
- 346 (8) Cole, J. J.; Prairie, Y. T.; Caraco, N. F.; McDowell, W. H.; Tranvik, L. J.; Striegl, R.
347 G.; Duarte, C. M.; Kortelainen, P.; Downing, J. a.; Middelburg, J. J.; Melack, J.
348 Plumbing the Global Carbon Cycle: Integrating Inland Waters into the Terrestrial
349 Carbon Budget. *Ecosystems* **2007**, *10* (1), 172–185.
350 <https://doi.org/10.1007/s10021-006-9013-8>.

- 351 (9) Battin, T. J.; Kaplan, L. A.; Findlay, S.; Hopkinson, C. S.; Marti, E.; Packman, A. I.;
352 Newbold, J. D.; Sabater, F. Biophysical Controls on Organic Carbon Fluxes in
353 Fluvial Networks. *Nat. Geosci.* **2008**, *1* (2), 95–100.
354 <https://doi.org/10.1038/ngeo101>.
- 355 (10) Fasching, C.; Behounek, B.; Singer, G.; Battin, T. J. Microbial Degradation of
356 Terrigenous Dissolved Organic Matter and Potential Consequences for Carbon
357 Cycling in Brown-Water Streams. *Sci. Rep.* **2014**, *4*, 4981.
358 <https://doi.org/10.1038/srep04981>.
- 359 (11) Panneer Selvam, B.; Lapierre, J.-F.; Soares, A. R. A.; Bastviken, D.; Karlsson, J.;
360 Berggren, M. Photo-Reactivity of Dissolved Organic Carbon in the Freshwater
361 Continuum. *Aquat. Sci.* **2019**, *81* (4), 57. [https://doi.org/10.1007/s00027-019-0653-](https://doi.org/10.1007/s00027-019-0653-0)
362 [0](https://doi.org/10.1007/s00027-019-0653-0).
- 363 (12) Bostick, K. W.; Zimmerman, A. R.; Goranov, A. I.; Mitra, S.; Hatcher, P. G.;
364 Wozniak, A. S. Photolability of Pyrogenic Dissolved Organic Matter from a Thermal
365 Series of Laboratory-Prepared Chars. *Sci. Total Environ.* **2020**, *724*, 138198.
366 <https://doi.org/10.1016/j.scitotenv.2020.138198>.
- 367 (13) Battin, T. J.; Besemer, K.; Bengtsson, M. M.; Romani, A. M.; Packmann, A. I. The
368 Ecology and Biogeochemistry of Stream Biofilms. *Nat. Rev. Microbiol.* **2016**, *14* (4),
369 251–263. <https://doi.org/10.1038/nrmicro.2016.15>.
- 370 (14) Norwood, M. J.; Louchouart, P.; Kuo, L. J.; Harvey, O. R. Characterization and
371 Biodegradation of Water-Soluble Biomarkers and Organic Carbon Extracted from
372 Low Temperature Chars. *Org. Geochem.* **2013**, *56*, 111–119.

- 373 <https://doi.org/10.1016/j.orggeochem.2012.12.008>.
- 374 (15) Myers-Pigg, A. N.; Louchouart, P.; Amon, R. M. W.; Prokushkin, A.; Pierce, K.;
375 Rubtsov, A. Labile Pyrogenic Dissolved Organic Carbon in Major Siberian Arctic
376 Rivers: Implications for Wildfire-Stream Metabolic Linkages. *Geophys. Res. Lett.*
377 **2015**, *42* (2), 377–385. <https://doi.org/10.1002/2014GL062762>.
- 378 (16) Judd, K. E.; Crump, B. C.; Kling, G. W. Variation in Dissolved Organic Matter
379 Controls Bacterial Production and Community Composition. *Ecology* **2006**, *87* (8),
380 2068–2079. [https://doi.org/10.1890/0012-9658\(2006\)87\[2068:vidomc\]2.0.co;2](https://doi.org/10.1890/0012-9658(2006)87[2068:vidomc]2.0.co;2).
- 381 (17) Freixa, A.; Ejarque, E.; Crognale, S.; Amalfitano, S.; Fazi, S.; Butturini, A.; Romaní,
382 A. M. Sediment Microbial Communities Rely on Different Dissolved Organic Matter
383 Sources along a Mediterranean River Continuum. *Limnol. Oceanogr.* **2016**, *61* (4),
384 1389–1405. <https://doi.org/10.1002/lno.10308>.
- 385 (18) Ateia, M.; Apul, O. G.; Shimizu, Y.; Muflihah, A.; Yoshimura, C.; Karanfil, T.
386 Elucidating Adsorptive Fractions of Natural Organic Matter on Carbon Nanotubes.
387 *Environ. Sci. Technol.* **2017**, *51* (12), 7101–7110.
388 <https://doi.org/10.1021/acs.est.7b01279>.
- 389 (19) Castan, S.; Sigmund, G.; Hüffer, T.; Tepe, N.; von der Kammer, F.; Chefetz, B.;
390 Hofmann, T. The Importance of Aromaticity to Describe the Interactions of Organic
391 Matter with Carbonaceous Materials Depends on Molecular Weight and Sorbent
392 Geometry. *Environ. Sci. Process. Impacts* **2020**, *22* (9), 1888–1897.
393 <https://doi.org/10.1039/D0EM00267D>.

- 394 (20) Lemire, J. A.; Harrison, J. J.; Turner, R. J. Antimicrobial Activity of Metals:
395 Mechanisms, Molecular Targets and Applications. *Nat. Rev. Microbiol.* **2013**, *11*
396 (6), 371–384. <https://doi.org/10.1038/nrmicro3028>.
- 397 (21) Sigmund, G.; Jiang, C.; Hofmann, T.; Chen, W. Environmental Transformation of
398 Natural and Engineered Carbon Nanoparticles and Implications for the Fate of
399 Organic Contaminants. *Environ. Sci. Nano* **2018**, *5* (11), 2500–2518.
400 <https://doi.org/10.1039/C8EN00676H>.
- 401 (22) Smith, H. G.; Sheridan, G. J.; Lane, P. N. J.; Nyman, P.; Haydon, S. Wildfire Effects
402 on Water Quality in Forest Catchments: A Review with Implications for Water
403 Supply. *J. Hydrol.* **2011**, *396* (1–2), 170–192.
404 <https://doi.org/10.1016/j.jhydrol.2010.10.043>.
- 405 (23) Fuß, T.; Behounek, B.; Ulseth, A. J.; Singer, G. A. Land Use Controls Stream
406 Ecosystem Metabolism by Shifting Dissolved Organic Matter and Nutrient
407 Regimes. *Freshw. Biol.* **2017**, *62* (3), 582–599. <https://doi.org/10.1111/fwb.12887>.
- 408 (24) Weishaar, J. L.; Aiken, G. R.; Bergamaschi, B. A.; Fram, M. S.; Fujii, R.; Mopper,
409 K. Evaluation of Specific Ultraviolet Absorbance as an Indicator of the Chemical
410 Composition and Reactivity of Dissolved Organic Carbon. *Environ. Sci. Technol.*
411 **2003**, *37* (20), 4702–4708. <https://doi.org/10.1021/es030360x>.
- 412 (25) Parlanti, E.; Wörz, K.; Geoffroy, L.; Lamotte, M. Dissolved Organic Matter
413 Fluorescence Spectroscopy as a Tool to Estimate Biological Activity in a Coastal
414 Zone Submitted to Anthropogenic Inputs. *Org. Geochem.* **2000**, *31* (12), 1765–
415 1781. [https://doi.org/10.1016/S0146-6380\(00\)00124-8](https://doi.org/10.1016/S0146-6380(00)00124-8).

- 416 (26) McKnight, D. M.; Boyer, E. W.; Westerhoff, P. K.; Doran, P. T.; Kulbe, T.; Andersen,
417 D. T. Spectrofluorometric Characterization of Dissolved Organic Matter for
418 Indication of Precursor Organic Material and Aromaticity. *Limnol. Oceanogr.* **2001**,
419 *46* (1), 38–48. <https://doi.org/10.4319/lo.2001.46.1.0038>.
- 420 (27) Murphy, K. R.; Stedmon, C. A.; Graeber, D.; Bro, R. Fluorescence Spectroscopy
421 and Multi-Way Techniques. PARAFAC. *Anal. Methods* **2013**, *5* (23), 6557.
422 <https://doi.org/10.1039/c3ay41160e>.
- 423 (28) Pucher, M.; Wünsch, U.; Weigelhofer, G.; Murphy, K.; Hein, T.; Graeber, D.
424 StaRdom: Versatile Software for Analyzing Spectroscopic Data of Dissolved
425 Organic Matter in R. *Water* **2019**, *11* (11), 2366.
426 <https://doi.org/10.3390/w11112366>.
- 427 (29) Pucher, M.; Graeber, D. StaRdom: PARAFAC Analysis on DOM EEMs, Calculating
428 Absorbance Slopes. <https://github.com/MatthiasPucher/StaRdom>. 2019.
- 429 (30) Stark, S.; Männistö, M. K.; Eskelinen, A. Nutrient Availability and PH Jointly
430 Constrain Microbial Extracellular Enzyme Activities in Nutrient-Poor Tundra Soils.
431 *Plant Soil* **2014**, *383* (1–2), 373–385. <https://doi.org/10.1007/s11104-014-2181-y>.
- 432 (31) Ylla, I.; Peter, H.; Romaní, A. M.; Tranvik, L. J. Different Diversity-Functioning
433 Relationship in Lake and Stream Bacterial Communities. *FEMS Microbiol. Ecol.*
434 **2013**, *85* (1), 95–103. <https://doi.org/10.1111/1574-6941.12101>.
- 435 (32) Sinsabaugh, R. L.; Follstad Shah, J. J. Ecoenzymatic Stoichiometry of Recalcitrant
436 Organic Matter Decomposition: The Growth Rate Hypothesis in Reverse.

- 437 *Biogeochemistry* **2011**, *102* (1–3), 31–43. <https://doi.org/10.1007/s10533-010->
438 9482-x.
- 439 (33) Romaní, A. M.; Guasch, H.; Munoz, I.; Ruana, J.; Vilalta, E.; Schwartz, T.; Emtiazi,
440 F.; Sabater, S. Biofilm Structure and Function and Possible Implications for Riverine
441 DOC Dynamics. *Microb. Ecol.* **2004**, *47* (4), 316–328.
442 <https://doi.org/10.1007/s00248-003-2019-2>.
- 443 (34) Romaní, A. M.; Vázquez, E.; Butturini, A. Microbial Availability and Size
444 Fractionation of Dissolved Organic Carbon After Drought in an Intermittent Stream:
445 Biogeochemical Link Across the Stream–Riparian Interface. *Microb. Ecol.* **2006**, *52*
446 (3), 501–512. <https://doi.org/10.1007/s00248-006-9112-2>.
- 447 (35) Sinsabaugh, R. L.; Follstad Shah, J. J.; Hill, B. H.; Elonen, C. M. Ecoenzymatic
448 Stoichiometry of Stream Sediments with Comparison to Terrestrial Soils.
449 *Biogeochemistry* **2012**, *111* (1–3), 455–467. <https://doi.org/10.1007/s10533-011->
450 9676-x.
- 451 (36) Romaní, A. M.; Fischer, H.; Mille-lindblom, C.; Tranvik, L. J.; Roman, A. M.; Fischer,
452 H.; Mille-lindblom, C.; Tranvik, L. J. Interactions of Bacteria and Fungi on
453 Decomposing Litter : Differential Extracellular Enzyme Activities. *Ecology* **2006**, *87*
454 (10), 2559–2569. <https://doi.org/10.1890/0012->
455 9658(2006)87[2559:IOBAFO]2.0.CO;2.
- 456 (37) Romani, A. M.; Sabater, S. Structure and Activity of Rock and Sand Biofilms in a
457 Mediterranean Stream. **2001**, *82* (11), 3232–3245.
458 <https://doi.org/https://doi.org/10.1890/0012->

- 459 9658(2001)082[3232:SAAORA]2.0.CO;2.
- 460 (38) Rasmussen, C. E.; Williams, C. K. I. Gaussian Processes for Machine Learning
461 (Adaptive Computation and Machine Learning). *MIT Press* **2005**.
- 462 (39) Stan Development Team. Stan Development Team (2019). RStan: The R Interface
463 to Stan. R Package Version 2.19.2. [Http://Mc-Stan.Org/](http://Mc-Stan.Org/). 2019.
- 464 (40) Fidel, R. B.; Laird, D. A.; Thompson, M. L.; Lawrinenko, M. Characterization and
465 Quantification of Biochar Alkalinity. *Chemosphere* **2017**, *167*, 367–373.
466 <https://doi.org/10.1016/j.chemosphere.2016.09.151>.
- 467 (41) Bodí, M. B.; Martin, D. A.; Balfour, V. N.; Santín, C.; Doerr, S. H.; Pereira, P.; Cerdà,
468 A.; Mataix-Solera, J. Wildland Fire Ash: Production, Composition and Eco-Hydro-
469 Geomorphic Effects. *Earth-Science Rev.* **2014**, *130*, 103–127.
470 <https://doi.org/10.1016/j.earscirev.2013.12.007>.
- 471 (42) Cairns, S.; Robertson, I.; Sigmund, G.; Street-Perrott, A. The Removal of Lead,
472 Copper, Zinc and Cadmium from Aqueous Solution by Biochar and Amended
473 Biochars. *Environ. Sci. Pollut. Res.* **2020**, *27* (17), 21702–21715.
474 <https://doi.org/10.1007/s11356-020-08706-3>.
- 475 (43) Bostick, K. W.; Zimmerman, A. R.; Wozniak, A. S.; Mitra, S.; Hatcher, P. G.
476 Production and Composition of Pyrogenic Dissolved Organic Matter From a Logical
477 Series of Laboratory-Generated Chars. *Front. Earth Sci.* **2018**, *6* (April), 1–14.
478 <https://doi.org/10.3389/feart.2018.00043>.
- 479 (44) Abiven, S.; Hengartner, P.; Schneider, M. P. W.; Singh, N.; Schmidt, M. W. I.

- 480 Pyrogenic Carbon Soluble Fraction Is Larger and More Aromatic in Aged Charcoal
481 than in Fresh Charcoal. *Soil Biol. Biochem.* **2011**, *43* (7), 1615–1617.
482 <https://doi.org/10.1016/j.soilbio.2011.03.027>.
- 483 (45) Engel, M.; Chefetz, B. Adsorptive Fractionation of Dissolved Organic Matter (DOM)
484 by Carbon Nanotubes. *Environ. Pollut.* **2015**, *197*, 287–294.
485 <https://doi.org/10.1016/j.envpol.2014.11.020>.
- 486 (46) Coble, P. G. Characterization of Marine and Terrestrial DOM in Seawater Using
487 Excitation-Emission Matrix Spectroscopy. *Mar. Chem.* **1996**, *51* (4), 325–346.
488 [https://doi.org/10.1016/0304-4203\(95\)00062-3](https://doi.org/10.1016/0304-4203(95)00062-3).
- 489 (47) Coble, P. G.; Green, S. A.; Blough, N. V.; Gagosian, R. B. Characterization of
490 Dissolved Organic Matter in the Black Sea by Fluorescence Spectroscopy. *Nature*
491 **1990**, *348* (6300), 432–435. <https://doi.org/10.1038/348432a0>.
- 492 (48) Murphy, K. R.; Ruiz, G. M.; Dunsmuir, W. T. M.; Waite, T. D. Optimized Parameters
493 for Fluorescence-Based Verification of Ballast Water Exchange by Ships. *Environ.*
494 *Sci. Technol.* **2006**, *40* (7), 2357–2362. <https://doi.org/10.1021/es0519381>.
- 495 (49) Fellman, J. B.; Hood, E.; Spencer, R. G. M. Fluorescence Spectroscopy Opens
496 New Windows into Dissolved Organic Matter Dynamics in Freshwater Ecosystems:
497 A Review. *Limnol. Oceanogr.* **2010**, *55* (6), 2452–2462.
498 <https://doi.org/10.4319/lo.2010.55.6.2452>.
- 499 (50) Singh, S.; Inamdar, S.; Scott, D. Comparison of Two PARAFAC Models of
500 Dissolved Organic Matter Fluorescence for a Mid-Atlantic Forested Watershed in

- 501 the USA. *J. Ecosyst.* **2013**, 2013, 1–16. <https://doi.org/10.1155/2013/532424>.
- 502 (51) Yamashita, Y.; Fichot, C. G.; Shen, Y.; Jaffé, R.; Benner, R. Linkages among
503 Fluorescent Dissolved Organic Matter, Dissolved Amino Acids and Lignin-Derived
504 Phenols in a River-Influenced Ocean Margin. *Front. Mar. Sci.* **2015**, 2 (NOV), 1–14.
505 <https://doi.org/10.3389/fmars.2015.00092>.
- 506 (52) Romani, A. M.; Artigas, J.; Ylla, I. Extracellular Enzymes in Aquatic Biofilms:
507 Microbial Interactions versus Water Quality Effects in the Use of Organic Matter.
508 *Microb. biofilms* **2012**, 153–174.
- 509 (53) Arnosti, C.; Bell, C.; Moorhead, D. L.; Sinsabaugh, R. L.; Steen, A. D.; Stromberger,
510 M.; Wallenstein, M.; Weintraub, M. N. Extracellular Enzymes in Terrestrial,
511 Freshwater, and Marine Environments: Perspectives on System Variability and
512 Common Research Needs. *Biogeochemistry* **2014**, 117 (1), 5–21.
513 <https://doi.org/10.1007/s10533-013-9906-5>.
- 514 (54) Kleber, M. What Is Recalcitrant Soil Organic Matter? *Environ. Chem.* **2010**, 7 (4),
515 320. <https://doi.org/10.1071/EN10006>.
- 516 (55) Luo, Z.; Wang, E.; Sun, O. J. A Meta-Analysis of the Temporal Dynamics of Priming
517 Soil Carbon Decomposition by Fresh Carbon Inputs across Ecosystems. *Soil Biol.*
518 *Biochem.* **2016**, 101, 96–103. <https://doi.org/10.1016/j.soilbio.2016.07.011>.